Journal of Natural Gas Science and Engineering 38 (2017) 74–80

Contents lists available at ScienceDirect

Journal of Natural Gas Science and Engineering

journal homepage: www.elsevier.com/locate/jngse

Quantitative evaluation of the heterogeneity for tight sand based on the nuclear magnetic resonance imaging

Xinmin Ge [a, b, *], Yiren Fan [a, b], Yufeng Xiao [c], Jianyu Liu [a], Donghui Xing [a], Dingna Gu [d], Shaogui Deng [a, b]

[a] School of Geosciences in China University of Petroleum, Qingdao, Shandong, China
[b] Laboratory for Marine Mineral Resources, Qingdao National Laboratory for Marine Science and Technology, Qingdao, Shandong, China
[c] Research Institute of Petroleum Exploration & Development-Langfang, Langfang, Hebei, China
[d] Tuha Business Division, China Petroleum Logging CO. LTD., Shanshan, Xinjiang, China

ARTICLE INFO

Article history:
Received 12 April 2016
Received in revised form
18 December 2016
Accepted 25 December 2016
Available online 27 December 2016

Keywords:
Tight sand
Nuclear magnetic resonance imaging
Variogram analysis
First order spherical model
Heterogeneity index
Genetic algorithm

ABSTRACT

Tight sand exhibits high degree of heterogeneity due to the complex pore structure. It is vital to evaluate the heterogeneity since it controls the fluid storage and transportation mechanisms, as well as geophysical responses. A novel method is put forward to quantify the heterogeneity based on the magnetic resonance imaging (MRI) experiments and the variogram analysis. Images of weight transversal relaxation times of fully water saturated core samples are acquired based on the spin echo sequence, slice-selecting pulse, frequency-coding pulse and phase-coding pulse and two dimensional discrete fast Fourier transform (2D-FFT). In addition, variogram function of the first order spherical model and the genetic algorithm are implemented to characterize the heterogeneity of pore distributions along vertical and horizontal directions. Furthermore, relationships between the average heterogeneity index and the tortuosity, and the mercury withdrawal efficiency, are also investigated to reveal the physical meaning of the heterogeneity index we presented. The result shows that the average heterogeneity index is positively correlated with the tortuosity index and negatively correlated with the mercury withdrawal efficiency. Our study provides an effective way to investigate the spatial heterogeneity of pore space, which serves as an important source of information for core analysis and formation evaluation.

© 2016 Elsevier B.V. All rights reserved.

1. Introduction

Tight sand has very low porosity and low permeability (with in-situ matrix permeability lower than 0.1mD), complex pore structure and high heterogeneity, which brings great difficulties in characterization and evaluation of such reservoirs (Rezaee et al., 2012; Li et al., 2015; Zhao et al., 2015a, 2015b; He et al., 2016; Ou et al., 2016). It is vital to investigate the pore structure, pore-matrix coupling relationship and heterogeneous degree of tight sand since some useful information such as petrophysical, reservoir and geophysical well logging parameters are strongly affected by the pore structure and its heterogeneous degree (Zhao et al., 2016; Sun et al., 2016). There are many existing techniques to investigate the pore size distributions of tight sand, including thin section, scanning electron microscope (SEM), mercury injection capillary pressure (MICP) and low field nuclear magnetic resonance (NMR). Among these methods, NMR is featured as a non-destructive and convenient technique which provides three dimensional pore size and fluid distributions of core samples. By detecting and inversing relaxation signals of hydrogen in pore space, we can obtain transversal relaxation time (T_2) and longitudinal relaxation time (T_1) spectrums, which are commonly used for pore structure characterization and estimation of porosity and permeability. Generally, there are two main categories of low field NMR experiments. The first is the NMR spectrum such as T_1 spectrum and T_2 spectrum, which helps us to recognize relaxation properties and quantify relaxation components. However, it cannot show the inter pore structure and heterogeneity for core samples at different slices. The second is the magnetic resonance imaging (MRI) such as the spin density image, T_1 and T_2 weighted images, which gives pore size distributions of core samples at different scales and locations,

* Corresponding author. School of Geosciences in China University of Petroleum, Qingdao, Shandong. China.
E-mail address: gexinmin2002@163.com (X. Ge).

http://dx.doi.org/10.1016/j.jngse.2016.12.037
1875-5100/© 2016 Elsevier B.V. All rights reserved.

facilitating investigations of pore distributions and fluid transportations.

Many studies are found to investigate the pore structure, multiphase percolation law, and other petroleum engineering problems with the help of MRI in recent decades (Xiao, 1995; Doughty and Tomutsa, 1997; Coussot, 1998; Issa et al., 1998; Balzarini et al., 2001; Nicula and Lyne, 2001; Belonogov et al., 2005; Pomerantz et al., 2008; Mitchell et al., 2013) However, most of the works published did not unveil the quantitative description of heterogeneity and some mathematical models cannot fit the experimental data effectively. We extended the application of MRI data (Pomerantz et al., 2008) to the tight sand samples in this study. The main aims of our work are twofold. The first component is to reveal the detailed procedures and algorithms of MRI and the second component is to propose a quantitative parameter to depict the heterogeneity of pore distributions.

2. Method

MRI achieves great development and is widely used in many fields such as physics, chemistry, biology, medical science and petroleum industry after the first image (Lauterbur, 1973; Mitchell et al., 1986). MRI introduces linear gradient field to make static magnetic fields inhomogeneous. The linear gradient of one direction (x direction) can be expressed as:

$$\mathbf{G_x} = \mathbf{x}\frac{\partial B_x}{\partial x} \tag{1}$$

where B_x and $\mathbf{G_x}$ are the outer magnetic field and the magnetic field gradient in x direction.

Along the gradient direction, different positions have their unique resonance frequencies, which can be expressed as:

$$\omega_x = \gamma(B_0 + \mathbf{x}\cdot\mathbf{G_x}) = \omega_0 + \Delta\omega \tag{2}$$

where B_0 is static magnetic field, γ is gyromagnetic ratio and ω_0 is Larmor frequency.

By Eq. (2) the spatial displacement is converted to frequency displacement and the location of sample can be fixed. Usually the magnetic field gradient is linear and can be stated as the form of the second order tensor:

$$\mathbf{G} = \begin{bmatrix} \mathbf{ii}\frac{\partial B_x}{\partial x} & \mathbf{ij}\frac{\partial B_x}{\partial y} & \mathbf{ik}\frac{\partial B_x}{\partial z} \\ \mathbf{ji}\frac{\partial B_y}{\partial x} & \mathbf{jj}\frac{\partial B_y}{\partial y} & \mathbf{jk}\frac{\partial B_y}{\partial z} \\ \mathbf{ki}\frac{\partial B_z}{\partial x} & \mathbf{kj}\frac{\partial B_z}{\partial y} & \mathbf{kk}\frac{\partial B_z}{\partial z} \end{bmatrix} \tag{3}$$

If the direction of static magnetic field is always towards z and the intensity of static magnetic field is greater than that of linear gradient field ($B_0 >> |\mathbf{B}|$), the linear gradient field in x ($\mathbf{x}B_x$) and y ($\mathbf{y}B_y$) directions can be omitted and Eq. (3) can be simplified as

$$\mathbf{G} = \frac{\partial B_z}{\partial x}\vec{\mathbf{k}}\cdot\vec{\mathbf{i}} + \frac{\partial B_z}{\partial y}\vec{\mathbf{k}}\cdot\vec{\mathbf{j}} + \frac{\partial B_z}{\partial z}\vec{\mathbf{k}}\cdot\vec{\mathbf{k}} \tag{4}$$

Assuming the gradient field only has values in x and y direction, Eq. (4) is transformed into

$$\mathbf{G} = \frac{\partial B_z}{\partial x}\vec{\mathbf{i}} + \frac{\partial B_z}{\partial y}\vec{\mathbf{j}} = \mathbf{G_x}\vec{\mathbf{i}} + \mathbf{G}_y\vec{\mathbf{j}} \tag{5}$$

The resonance frequency along the direction of magnetic field $\mathbf{G}$ can be expressed as

$$\omega_k = \gamma\mathbf{G}\cdot\mathbf{r} = \gamma(G_x x + G_y y) \tag{6}$$

If a 90°radio frequency (RF) pulse is added along x direction of rotary coordinate system, the spin located in the isochromatic surface will be motivated and the resonance signal is produced, and can be expressed in the time domain

$$S(t) = \int \rho(r)e^{i(w_0 - w) + \gamma G\cdot r)t}dr^3 \tag{7}$$

where $\rho(r)$ is the spin density.

Since the resonance frequency is linearly correlated with spatial coordinates, the spin density $\rho(r)$ can be obtained by inverse Fourier transform of $S(t)$. For the two dimensional case, Eq. (7) can be expressed as

$$S(t) = \int P(\omega_k)e^{i\omega_k t}d\omega_k \tag{8}$$

where $P(\omega_k) = \iint \rho_{\omega_k}(x,y)dxdy$ is the spin density projection and $\rho_{\omega_k}(x,y)$ is the spin density of the isochromatic surface.

Assuming the resonance frequency ω_k covers all sample surface, then we can get the projected contour profile in projection axis ω (parallel with gradient field $\mathbf{G}$) and the NMR image can be obtained by inverse Fourier transform of the projected contour profile.

3. Experiment

In this work, we used MacroMR (produced by Niumag Corporation) to carry out the experiments. The magnetic field intensity is approximately 0.3 T, the main frequency is 12.8 MHz and the diameter of the probe coil is 25.4 mm. Data is uniformly sampled with a total voxel of 512 × 512 for each slice and the length of each slice is 3 mm. The equipment uses the spin echo sequence. As shown in Fig. 1, G_s is the slice-selecting gradient pulse, G_p is the phase-coding gradient pulse and G_r is the frequency-coding gradient pulse. The exact position of core sample can be fixed (x, y and z coordinate) by three pulses. T_R is the recovery time which indicates the time interval between adjacent 90° RF pulses. T_E is the echo time, which is twice the time interval between the 90° RF pulse and the 180° RF pulse. Combing the 90°RF pulse and the slice-selecting gradient pulse, the slice is fixed and then the macroscopic magnetization vector is pulled down to XOY plane. After the time

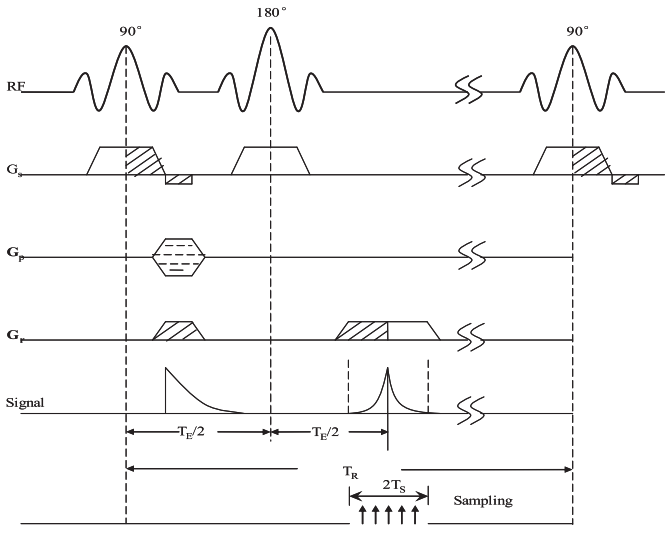

Fig. 1. Diagram of typical spin echo sequence.

Download English Version:

https://daneshyari.com/en/article/5485159

Download Persian Version:

https://daneshyari.com/article/5485159

Daneshyari.com